Reprinted from "Ecological Applications" Volume 12, number 1, 2002, pp. 218-237, Fonseca et al.: Modeling seagrass landscape pattern and associated ecological attributes. With permission from the Ecological Society of America.

Ecological Applications, 12(1), 2002, pp. 218–237
© 2002 by the Ecological Society of America

MODELING SEAGRASS LANDSCAPE PATTERN AND ASSOCIATED ECOLOGICAL ATTRIBUTES

MARK FONSECA,[1,5] PAULA E. WHITFIELD,[2] NINA M. KELLY,[3] AND SUSAN S. BELL[4]

[1]*Department of Integrative Biology, University of California, Berkeley, California 94720 USA*
[2]*National Oceanic and Atmospheric Administration, National Ocean Service, Center for Coastal Fisheries and Habitat Research, 101 Pivers Island Road, Beaufort, North Carolina 28516 USA*
[3]*Department of Environmental Science, Policy, and Management, Ecosystem Sciences Division, Berkeley College of Natural Resources, University of California, Berkeley, California 94720 USA*
[4]*Biology Department, University of South Florida, Tampa, FL 33620 USA*

Abstract. A predictive model for seagrass bed coverage (presence/absence at 1-m resolution) and ecological attributes of the bed, such as biomass and shoot density, would be a valuable management tool. But forming such a predictive model is complicated by a number of factors that strongly influence seagrass bed structure and our interpretation of its ecological function. The factors include the effects of waves and water depth (hydrodynamic setting) and the spatial and temporal scales of the sampling technique itself. In this study, we examined the coherence of predictions of seagrass cover and ecological attributes of temperate, mixed-species seagrass derived from two common sampling techniques, (video) line transect (commonly used by biologists) and grid-sampled surveys (often used in remote sensing). Mapping resolution was held constant at 1 m, and the two techniques applied across seagrass beds of varying coverage that reflected the effect of a hydrodynamic gradient ranging from patchy, high-energy beds to continuous cover, low-energy beds. We found that the prediction of seagrass coverage as a function of hydrodynamic setting can be improved not only by increasing the spatial extent of sampling at a fixed resolution (1 m), but also by ensuring that data for both dependent (e.g., percent cover) and independent (e.g., wave exposure) variables are averaged over similar scales (spatial extent and resolution). Large-scale features of the landscape, such as patches several meters in width, appeared to be best quantified by sampling over a large spatial extent, as with the video transects. Therefore, contiguous sampling over a broad spatial extent, as opposed to our numerous, somewhat smaller sampling (grid-sampled, 50 × 50 m areas) is the more appropriate strategy for predicting the probability of seagrass bed cover. Conversely, we found that ecological attributes of the seagrass bed (biomass, shoot density, and sediment composition) were best characterized by sampling over a shorter spatial extent (i.e., <50 m), indicating that very localized conditions may have influenced patterns of seagrass community attributes. Generalizing information about seagrass bed ecological attributes obtained from high-resolution samples (fine scale) taken over a broad spatial extent (coarse or landscape scale), as may occur with resource surveys and impact assessments, has the potential to be highly misleading, especially in patchy environments. The influence of sampling scale and survey method on the prediction of coverage and ecological attributes of seagrass beds reveals the need to carefully choose sampling designs to evaluate seagrass distribution and their associated ecological characteristics in the Beaufort, North Carolina (USA) area, and perhaps in other like habitats.

Key words: ecological attributes; hydrodynamics; landscape pattern; resource management; scale; seagrass; water depth; waves.

INTRODUCTION

The documentation of decreasing seagrass habitat in many areas worldwide (Cambridge et al. 1986, Robblee et al. 1991, Quammen and Onuf 1993) has resulted in efforts to quantify seagrass spatial distribution over large geographic areas, from 10 to 10^4 m. Aerial photography and, to a lesser degree, in situ mapping of seagrass distribution has been the focus of monitoring programs (Dobson et al. 1995) that ultimately seek to link changes in distribution to changes in ecological services (e.g., water filtration, nursery habitat) provided by the seagrass resource. Determining changes in distribution over time often involves comparing data collected from slightly different sites, sometimes using different sampling protocols (e.g., contrast Robbins and Bell [2000], 1-m resolution using walking surveys,

·Manuscript received 21 April 2000; revised 11 October 2000; accepted 21 November 2000; final version received 6 March 2001.

[5] Present address: National Oceanic and Atmospheric Administration, National Ocean Service, Center for Coastal Fisheries and Habitat Research, 101 Pivers Island Road, Beaufort, North Carolina 28516 USA.
E-mail: mark.fonseca@noaa.gov

with Ferguson and Korfmacher [1997], ~17-m resolution using satellites). Likewise, data on seagrass coverage is often collected at different scales, where scale can be considered to be composed of both spatial extent and resolution within that extent and may also be employed to assess seagrass changes.

The limitations involved in cross-scale comparisons have alone been shown to be problematic in the field of ecology and have been the subject of previous studies (e.g., Rastetter et al. 1992). Cross-scale comparisons may be particularly vexing when resource managers utilize results founded upon studies conducted at fine scales (~1–10 m) to address problems occurring across coarse, landscape scales (e.g., $10–10^3$ m). Unfortunately, comparisons among different sampling techniques are rarely conducted at the landscape scale. To our knowledge, there are no comparative studies of landscape-scale sampling protocols in seagrass ecosystems. Although some work regarding variation in plant coverage and ecological functions in seagrass systems has been examined on landscape scales (Patriquin 1975, Hine et al. 1987, Kirkman and Kuo 1990, Turner et al. 1999, Robbins and Bell 2000), many more studies have focused on seagrass bed structure and functions over areas far less than 100 m^2 (Ginsberg and Lowenstam 1958, Zieman 1972, Orth 1977, Kenworthy et al. 1982, Fonseca et al. 1983, Valentine et al. 1994, Irlandi et al. 1995, Irlandi 1996). It is generally not known whether the results of the fine-scale studies can be extrapolated to predict characteristics of these habitats (but see Bell et al. 1994 and Turner et al. 1999). Moreover, we are only beginning to assess the response of seagrass systems to perturbations at the much larger scales (Robbins and Bell 1994, Fonseca 1996*b*, Bell and Hall 1997, Fonseca et al. 2000*b*) that are relevant to management concerns regarding habitat extent and the ecological services they provide (e.g., such as nursery role, sediment stability, water column filtration, and nutrient cycling; Bell et al. 1997).

In order to choose a sampling strategy and predict seagrass landscape patterns at various spatial scales, it is important to understand the processes influencing the expression of those patterns. Physical disturbance via hydrodynamic activity is widely acknowledged to have primary influence over the spatial and temporal dynamics of seagrass beds (see Fonseca 1996*a*). In habitats exposed to rapidly flowing water, seagrass beds form patchy, dune-like structures, whereas in quiescent areas, seagrass beds have low relief and nearly continuous cover (Patriquin 1975, Fonseca et al. 1983, Kirkman and Kuo 1990, Marba and Duarte 1995, Fonseca 1996*b*, Fonseca and Bell 1998). Recently, in North Carolina, Fonseca and Bell (1998) demonstrated the existence of strong correlative relationships between hydrodynamic setting (tidal current speed, water depth, and exposure to waves) and a wide variety of ecological attributes including seagrass biomass, abundance, patch geometry, and sediment characteristics. Similarly, in freshwater systems, the relationship between water depth, bottom slope, fetch, soil type, disturbance, and plant community structure has been modeled, also with the goal of predicting macrophyte growth and distribution (Narumalani et al. 1997). Both these studies provide the kinds of data that have been shown to successfully describe statistical relationships among environmental variables that can be scaled up from small to larger areas for resource conservation planning (Franklin 1995).

The importance of accurately delineating landscape-level features in seagrass ecosystems was recently demonstrated by Turner et al. (1999) who found that seagrass landscape variables (e.g., fractal dimension and nearest neighbor distance) and wave exposure together explained 62.5% of the variance in faunal species abundance among seagrass habitats. Similarly, Fonseca (1996*b*) reported that bathymetry in seagrass landscapes was scale dependent (i.e., variance in water depth changed as a function of the distance between samples) within the 50 × 50 m study areas used by Fonseca and Bell (1998). Unless scaling limitations of these data are understood, the degree to which we can generalize ecological information collected in seagrass beds will be severely limited. Such predictions cannot be achieved until the range of scale dependence is established and a sampling protocol employed to capture that scale of spatial variance. It is equally important for effective management to understand how different sampling protocols influence these conclusions (e.g., whether they satisfy parametric sampling requirements such as independence among replicates; Fonseca 1996*b*).

To address these issues of sampling strategy, we examined whether sampling of seagrass bed cover and various ecological attributes of these beds, when performed over the same areas and using two common but different landscape-scale sampling strategies (line transect vs. grid sampling), might lead to divergent conclusions. We also explored ways in which our predictive abilities might be enhanced through the inclusion of additional physical information into the modeling process. Specifically, three different problems were investigated. First, differences between two survey types (grid-sampled and video transect) were assessed and the survey data examined for their relation to physical setting (water depth and wave-driven hydrodynamics) over varying spatial extent. Second, sampling of several ecological attributes was conducted in association with the two survey types; the relation of these attributes with physical setting was assessed. Finally, an examination of the potential effect of shoaling on predictions of seagrass cover and ecological attributes was conducted on a limited portion of the study area in order to test its influence on our ability to predict cover and ecological attributes of the seagrass bed.

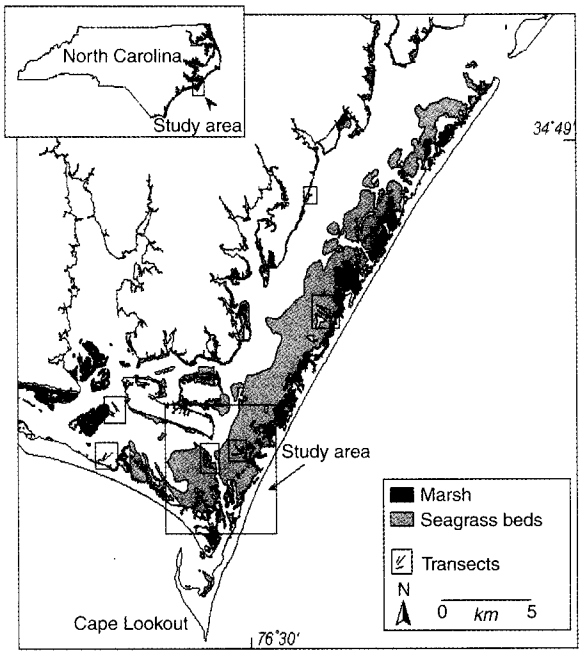

FIG. 1. Regional map of Core and Back Sounds, Carteret County, North Carolina, USA, showing the location of the video transects and the 18 previously surveyed 50 × 50 m grid sample study locations (Fonseca and Bell 1998). Boxes depict the size and orientation of the geographic-information-system-derived relative (wave) exposure index (REI) grids computed for the video transect study (variable box size but 100 × 100 m resolution within). Note that two video transect sites occur within the same REI box off the southwest corner of Harker's Island. The study-area box refers to the *Shoaling effects* section. Distributions of marsh and seagrass beds are from Ferguson et al. (1991).

METHODS

Background

Predictions of seagrass cover in relation to physical setting were obtained from previously studied (Fonseca and Bell 1998), 50 × 50 m grids in seagrass beds near Beaufort, North Carolina, USA surveyed in 1991–1992 (grid-sampled). These previous data were compared with new seagrass coverage data collected in 1995 from transect surveys using an underwater video camera (video transect) over and around several of the same study sites from 1991 to 1992. The video transect surveys covered distances >1000 m of spatial extent, necessitating sampling from around, and not just within, the 50 × 50 m grids. For both data types (grid-sampled and video transect), resolution was kept the same (1 m) while the spatial extent and geometry of the samples were different between the two survey methods.

Seagrass cover modeling (1-m resolution over varying spatial extent)

Site selection.—The seven sites chosen for this study included six used during previous studies (Bell et al. 1994, Murphey and Fonseca 1995, Fonseca 1996*b*, Fonseca and Bell 1998, Townsend and Fonseca 1998). These sites were spread across ~22 km of the estuary (Fig. 1) and were chosen to represent the full range of wave exposure values reported by Fonseca and Bell (1998). Some sites were not near any emergent shorelines and experienced a wave climate that built over a long (>15 km) fetch (i.e., high energy) (see Plate 1). At the other extreme, some sites occurred immediately adjacent to emergent *Spartina alterniflora* marsh and had virtually no fetch (i.e., low energy). All sites were within 10 km of an ocean inlet. Consequently, salinities ranged between 30 and 34 ppt (on a mass per mass basis) while annual temperature ranged from ~4 to 33°C (NOS/NOAA, Beaufort Laboratory, *unpublished data*).

Relative wave exposure index.—Wave exposure for our sites in southern Core Sound and Back Sound, North Carolina (34°49′–34°50′ N, 76°20′–76°40′ W) were computed using a relative (wave) exposure index (REI) modified from Keddy (1982). The index was the same as that performed manually by Murphey and Fonseca (1995) and Fonseca and Bell (1998) but was computed here using a macro written in Arc/INFO version 8.0.1 (a geographic information system; Environmental Systems Research Institute, Redlands, California, USA) to solve the following equation:

$$\mathrm{REI} = \sum_{i=1}^{8} (V_i \times P_i \times F_i) \qquad (1)$$

where: i = ith compass heading (1–8 [north, northeast, east, etc.], in 45° increments), V = average monthly maximum wind speed in meters per second, P = percentage of frequency with which wind occurred from the ith direction, and F = effective fetch in meters. Wind data were obtained as hourly observations of speed and direction for the three years preceding each study period (1991–1992 and 1995) from an NOAA monitoring station at Cape Lookout, North Carolina, a site within ~10 km of all our sampling sites. Fetch was defined as the distance from the site to land along a given compass heading. Effective fetch was computed by measuring fetch along four lines radiating out from either side of the ith compass heading at increments of 11.25°, including the ith heading (n = 9). Effective fetch was then calculated by summing the product of the fetch × cosine of the angle of departure from the ith heading over each of the nine lines and dividing by the sum of the cosine of all the angles. This weighting of multiple fetch measures for each compass heading helps account for irregularities in shoreline geometry that could misrepresent the potential of wind wave development from a given compass heading (Shore Protection Manual 1977).

Video transect data.—Transect locations were chosen to remain within seagrass habitat in and around the aforementioned sites. This was accomplished by inspecting recent aerial photographs (L. Wood, National

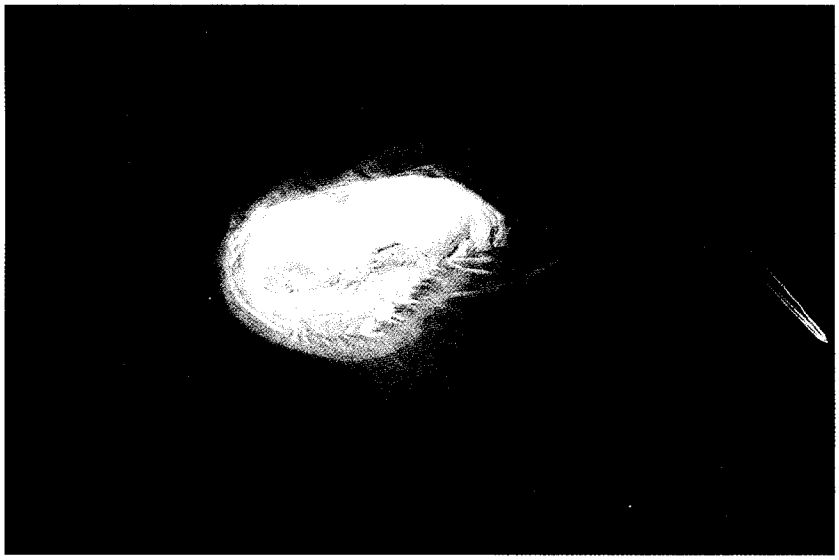

PLATE 1. Aerial photograph of the Dredge Island looking north, taken in 1989. The patchy nature of the seagrass beds is clearly evident around the island. As additional dredged material has been added to the island for the maintenance of the adjacent channel (running along the northeast side of the island where the vessel wake is visible), the island has created a wind shadow to the southwest, blocking the high wave energy that is generated from the northeast direction. The seagrass beds in the lower left of the photo (the southwest side) are no longer patchy but have fully coalesced as they have been released from the disturbance effects of the northeasterly wave events. Photograph by M. Fonseca.

Marine Fisheries Service, NOAA, Beaufort, North Carolina, USA, *personal communication*) and previous seagrass mapping from aerial photography (Ferguson et al. 1991). At each site, three transects were established (Table 1). Sections of the transects sometimes passed through small portions of Fonseca and Bell's (1998) 50 × 50 m grids but at angles oblique to the original site layout, which, together with a georectification accuracy of approximately ±2.0 m, precluded direct, pixel by pixel comparison of the two data sets.

TABLE 1. Summary statistics of video transect length (in meters) and mean, minimum, and maximum relative (wave) exposure index (REI). Sites were located in Southern Core Sound and Back Sound, North Carolina, USA, between 34°49′ N and 34°50′ N and between 76°20′ W and 76°40′ W.

Site	Transect	Video transect length	Mean REI	Minimum REI	Maximum REI
BR2	1	521	2.17	1.81	2.35
BR2	2	427	2.14	2.04	2.35
BR2	3	774	2.11	1.91	2.60
DAVIS	1	180	5.17	5.09	5.32
DAVIS	2	207	5.08	4.33	5.32
DAVIS	3	141	4.57	4.33	5.13
HIH1	1	935	4.54	2.60	5.67
HIH1	2	1307	4.49	2.88	5.49
HIH1	3	802	4.28	2.88	5.16
HI2	1	1161	4.58	3.70	6.24
HI2	2	944	4.73	3.69	5.44
HI2	3	1047	4.45	2.39	5.43
HIH2	1	657	4.88	0.09	6.24
HIH2	2	571	4.89	2.36	5.75
HIH2	3	587	4.90	0.09	6.03
MMN	1	317	2.66	2.51	2.75
MMN	2	361	2.59	1.93	2.77
MMN	3	399	2.65	2.37	2.91
NR1	1	725	2.73	2.56	2.96
NR1	2	623	2.64	2.55	2.77
NR1	3	572	2.70	2.55	2.96

Between June and November 1995, seagrass coverage and water depth data were collected once only from each transect at the aforementioned seven sites (Fig. 1). Days with gentle winds near flood tide (low current speeds) were selected for video towing in order to ensure good water clarity for video and to minimize vessel drift; as a consequence, once set on course, tows appeared to be quite straight.

Two types of data were recorded for each successive 1-m distance along each video transect: (1) presence/absence of seagrass and (2) water depth (for a summary of the methods see Table 2). The video data were collected using a Sony 8-mm camcorder (Model CCD TR30; Sony, SKZ Kisarazu, Japan) in an underwater housing bolted to a roller trawl (Murphey and Fonseca 1995). The camera was mounted at a 45° angle relative to the sea floor. The field of view from the camera was set to be 1 m along the transect × 0.5 m in width. To collect water depth data, a Druck model PDCR 10/D pressure sensor (Druck, New Fairfield, Connecticut, USA) was also added to the roller trawl at a fixed distance 39 cm above the seafloor; this height was added to all depth values. The pressure sensor was connected by a cable to an onboard Campbell Scientific 21 × Micrologger (Campbell Scientific, Logan, Utah) that was programmed to collect depth data to the nearest 0.0001 m at either 5 or 3.3 Hz depending on the length of the transect and the available data logger

TABLE 2. Summary of methods used to model seagrass coverage and ecological attributes.

Data source	Seagrass coverage	Seagrass coverage: REI	Seagrass coverage: Water depth (MSL)	Ecological attributes	Ecological attributes: REI	Ecological attributes: Water depth (MSL)
Video transect data (1995)	Variable length underwater video transects at 1-m resolution	Arc/INFO macro grid at 100 × 100 m resolution	Pressure transducer on video sled at 1-m spatial resolution	Sampled from within 1-m^2 quadrats	Arc/INFO macro grid at 100 × 100 m resolution	Direct observation from within each quadrat
Grid-sampled data (Fonseca and Bell 1998)	Direct observation of 50 × 50 m grids at 1-m resolution	Arc/INFO macro single value for entire 50 × 50 m grid	Direct observation at 1-m spatial resolution	Sampled from within 1-m^2 quadrats	Arc/INFO macro single value for entire 50 × 50 m grid	Direct observation from within each quadrat

Notes: REI = relative (wave) exposure index; MSL = mean sea level.

storage capacity. These data were corrected to mean sea level (MSL) using NOAA tide models. The entire video system was weighted and towed slowly (~0.5 m/s) on the seafloor along the transects from a small motor vessel.

Latitude and longitude of each transect beginning and end points were collected with a Trimble Pathfinder 5000 GPS Rover (Trimble Navigation, Sunnyvale, California, USA). In order to maintain ~2-m accuracy at each location, at least 180 values were collected with the position dilution of precision (PDOP) set at 4 and an elevation mask of 15°. Data from a georeferenced base station located at the Beaufort Laboratory, calibrated to collect one position every 5 s, were used to perform a postmission differential correction of each of the 180 data points collected per transect endpoint. These values were then averaged, bringing the Rover data accuracy for each transect endpoint to within 2 m of its true position (August et al. 1994).

Each video transect line was broken into successive points at 1-m increments (point video transect) in Arc/INFO. In order to assign REI values to each point along the video transects, a rectangular area that included all transects at a site was arbitrarily delineated in Arc/INFO and used to generate a coverage of regularly spaced points, each centered at 100-m intervals. This REI grid had a pixel resolution of ×100 m (1 ha). Relative (wave) exposure index values were then computed for each of the 100 pixels centered over each grid point. The point video transects were then overlaid onto the REI grid using Arc/INFO, and the REI value for that 1-ha area was assigned to each point along the video transect that fell within the corresponding 1-ha area. Thus, each point location along the transect became a point sample of REI and seagrass coverage (presence/absence). All geographic data layers were projected in the State Plane coordinate system using the NAD83 datum with units equal to meters.

To obtain seagrass coverage data, the videotape was examined in the laboratory on a television screen and the presence or absence of seagrass was recorded for every successive meter of sea floor along each transect. Each successive meter of sea floor was viewed and ranked as "occupied" if >50% of the area was filled with seagrass after accounting for parallax. There were very few (estimated <1%) near-ties using this classification because of abrupt boundaries between seagrass and unvegetated seafloor. Because *Halodule wrightii* and *Zostera marina* intermingle at the submeter scale in this area, no distinction as to species was made during mapping. These presence/absence data were then merged with the MSL-corrected depth data downloaded from the Campbell data logger to yield a final data set with observations of REI, presence/absence of seagrass cover, and MSL water depth for each successive meter along each transect in Arc/INFO.

Grid data (50 × 50 m grids).—These data were derived from Fonseca and Bell (1998); a brief review of the methodology follows (see also Table 2). Mapping to generate the data for Fonseca and Bell (1998) was conducted four times, in May and November 1991 and June and November 1992, after selecting the general location of the study site from 1 : 24 000 aerial photographs. Mapping of 9 of the original 18 50 × 50 m sites had continued every spring and fall from 1992 to spring of 1995, which included six of the seven study sites surveyed with video in the present study. Because 3 yr had elapsed since the earlier study, we compared the relationship of seagrass cover to REI from the 1995 spring survey of the 50 × 50 m sites with that performed previously in 1991–1992 to verify that the same general relationship of cover to REI existed. This last task was critical to determine if the relationship was consistent with that of Fonseca and Bell (1998) and whether direct comparison of the data with the 1995 video transect data would be appropriate.

The actual position and orientation of the 50 × 50 m grids used by Fonseca and Bell (1998) were chosen haphazardly within portions of the seagrass landscape that visually appeared to have a consistent pattern of cover extending well beyond the boundaries of each study site. Each 50 × 50 m site was broken into a grid with points centered every 1 m. The 1-m^2 area around each point was visually surveyed for presence/absence

TABLE 3. Summary of analyses (see *Methods*) used to process information from various data sources, cross-referenced with *Methods* by analysis number.

Analysis	Model parameter(s) and sampling description	REI	Water depth (MSL)	Analytical method
I	Probability of seagrass cover at 1-m resolution using all grid-sampled data (50 × 50 m sites)	Arc/INFO macro; single value for all points in 50 × 50 m grid	Direct observation at 1-m spatial resolution	Logistic multiple regression
II	Probability of seagrass cover at 1-m resolution using grid-sampled data from sites with REI > 3.0×10^6 and REI ≤ 3.0×10^6	Arc/INFO macro; single value for all points in 50 × 50 m grid	Direct observation at 1-m spatial resolution	
III	Probability of seagrass cover at 1-m resolution using all video transect data	Arc/INFO macro; single value for all points in 100 × 100 m area	Pressure transducer on video sled at 1-m spatial resolution	
IV	Probability of seagrass cover at 1-m resolution using all video transect data where REI > 3.0×10^6 and REI ≤ 3.0×10^6	Arc/INFO macro; single value for all points in 100 × 100 m area	Pressure transducer on video sled at 1-m spatial resolution	
V	Probability of seagrass cover at 1-m resolution using combined grid-sampled and video transect data	Combined I and III, respectively	Combined I and III, respectively	
VI	Probability of seagrass cover at 1-m resolution using combined grid-sampled and video transect data where REI > 3.0×10^6 and REI ≤ 3.0×10^6	Combined II and IV, respectively	Combined II and IV, respectively	
VII	Percent seagrass cover computed over video transect segments within REI pixels and entire 50 × 50 m grid-sampled areas	Combined I and III, respectively	n/a	Linear regression
VIII	Scale dependence of video transect data, by transect	n/a	n/a	Semivariogram analysis
IX	Ecological attributes of seagrass beds along video transects	Arc/INFO macro; single value for each quadrat	Direct observation within quadrat	Regression, one-way ANOVA, PCA
X	Shoaling effects: probability of seagrass cover at 1-m resolution using all video transect data as well as video transect data where REI > 3.0×10^6; ecological attributes of seagrass beds along video transects	Combined I, III, and VIII	Combined I, III, and VIII	Combined I and IX

Note: REI = relative (wave) exposure index; MSL = mean sea level; PCA = principal components analysis; n/a = not applicable.

of seagrass using the same criteria as for the video transects (>50% cover = seagrass present). Water depth was recorded to the nearest decimeter at every 1-m increment, but only for every third row in the 50 × 50 m grid, beginning November 1991. Water depth was corrected for tidal change during the course of the survey as well as the overall relation to MSL using NOAA tide tables. The coverage observations from each 1-m^2 area were all assigned the same REI value that was computed from a corner point of the 50 × 50 m grid.

Statistical treatment of coverage and water depth.— All statistical analyses were performed on data classified as belonging to areas of either high or low hydrodynamic energy (where high = REI ≥ 3×10^6; Fonseca and Bell 1998) or both high and low combined. Binary predictive models of seagrass cover (presence/absence) at 1-m resolution were then computed for both the high and low energy areas as well as both high and low combined, but by data type (video transect and grid-sampled; Analyses I–IV, Table 3), using logistic multiple regression. The regressions were computed following the method used by Narumalani et al. (1997):

$$\begin{aligned}\hat{p}(\text{grass present}) &= p(d = 1/x) \\ &= 1/(1 + \exp[(B_0 + B_1x_1 + B_2x_2B_3x_3)]) \quad (2)\end{aligned}$$

where d is the presence (1) or absence (0) of seagrass

cover at each 1-m increment along the seafloor, x_1, x_2, and x_3 are time (survey date), REI, and MSL-corrected water depth, respectively, and B_0, B_1, B_2, and B_3 are coefficients derived from logit regression. Logit regression was performed using SAS (1995) procedure LOGISTIC. Rank correlations were computed under SAS (1995) to assess the predictive ability of the model. An analysis of maximum likelihood estimates ($P >$ chi-square) was used to determine the significance of the two independent variables in predicting the contribution of time, REI, and MSL water depth to $\hat{p}$ under the stepwise logistic multiple regression. The effect of time was blocked by forcing it into the model. For Analyses I–VI (Table 3), the SAS procedure computed Somer's D, a rank correlation statistic that, like r^2, represents the association of the predicted probabilities vs. the observed responses.

After comparing the relative sampling effort between the two data types, it was found that, despite selecting the same general sites as previously studied, the video transect and grid-sampled data types tended to sample different portions of the REI and water depth ranges (see *Results*). This was viewed as an opportunity to explore whether a single model using all available data could produce a more robust prediction. Therefore, the two data collections (video transect and grid-sampled) were concatenated (n = 43 095). Logistic multiple regression was also applied to this concatenated data set and again solved for both the entire data set (Analysis V, Table 3) and high and low energy regimes alone (Analysis VI, Table 3) for comparison with similar regressions run on the separate video transect and grid-sampled data collections.

Because REI values were derived from 1-ha pixels and then assigned to successive 1-m point observations of coverage (1-m resolution) along the video transects, the scale of assessment by REI and coverage differed by two orders of magnitude. Mixing spatial scales among data types has been reported to sometimes cause errors in detecting interrelationships among variables (Rastetter et al. 1992, Schoch and Dethier 1996). Therefore, percent cover along the video transects was computed at the same scale as the REI computations by computing percent cover from using the 1-m^2 observations for the portions of a transect that lie within each 100 × 100 m REI pixel, yielding one measure of percent cover per REI datum. This was the same approach used to calculate a single percent cover value for each entire grid-sampled (50 × 50 m) site, to which a single REI value had been assigned. However, video transects sometimes only crossed a short segment of a 100 × 100 m REI pixel (despite the average distance within an REI pixel = 114 m), and on occasion, that segment encompassed an isolated seagrass patch. As a result, some of these short transect segments were assigned 100% cover values although the percent cover over the surrounding seafloor at the 100 × 100 m extent may have been quite low and the REI value, high. To minimize the effect of these few inflated percent cover estimates, seven REI categories were created (0–1, >1–2, >2–3, >3–4, >4–5, >5–6, >6; all × 10^6) and the mean percent cover was computed for each REI category within each data type and regressed on REI (Analysis VII, Table 3).

Semivariogram analysis.—In order to identify the spatial extent over which scale dependence of coverage estimates occurred in the video transect survey, semivariogram analysis was performed for all transects together, by site using the 1-m resolution coverage data. Data were coded as 0 for no cover and 1 for cover (GS+ 1994; Analysis VIII, Table 3). Data for grid-sampled sites had previously been analyzed for depth values; here it was reanalyzed using binary cover values. The lag value for these computations was set to 1 m. The distance at which variance in seagrass coverage stabilized on the semivariogram, the sill, was interpreted to represent the spatial extent of scale-dependent changes in seagrass cover (Fonseca 1996*b*).

Ecological attributes of seagrass beds derived from point sampling (1 m^2)

Video transects.—In spring and fall of 1995, throw-trap samples were taken along the video transects at locations near to the midpoint of the transect segment as it passed through 100 × 100 m REI pixels. A 1-m^2 quadrat was thrown onto the nearest vegetated portion of the seafloor (see Table 2). Above- and belowground seagrass biomass, seagrass shoot density, and sediment silt-clay and organic matter content (top 3 cm) were collected from within these 1-m^2 quadrats for a total of 38 samples per each of two seasons. Temperature, salinity, and water depth were also recorded at each quadrat. All sampling gear and processing methods were the same as previous studies using this sampling gear (Bell et al. 1994, Fonseca et al. 1996, Fonseca and Bell 1998).

Grid-sampled.—One square meter quadrats were also used previously to survey ecological attributes of the grid-sampled sites (Fonseca and Bell 1998). The three quadrat samples from each of the 18 50 × 50 m grids were collected at four dates (June and September, 1991 and 1992), and each random quadrat location was rejected if it did not land on seagrass. The relationship of seagrass biomass, shoot density, and sediment characteristics to hydrodynamic setting derived from these point samples associated with the video transects were compared with that previously derived from the grid-sampled sites (Fonseca and Bell 1998).

Data analysis.—In order to assess the relationship of these ecological attributes with physical setting, the REI value for each point-sample (quadrat) was assigned that of the overlying, 1-ha resolution REI pixel, previously computed for video transects. The three quadrats deployed in each of the 50 × 50 m grids were all assigned the same REI value that was computed using a corner point of the 50 × 50 m grid (Tables 1 and 2),

but these replicate quadrats were averaged, yielding one attribute observation per REI value in order for replication to be congruent with the video transect data. Values for the ecological attributes seagrass shoot density, aboveground biomass, belowground biomass, and percentage of organic content of the sediment were all averaged on a square meter basis, based on three subsamples taken within each 50 × 50 m grid.

The relationships among the four ecological attributes and REI were examined after categorization into either high or low hydrodynamic regime and compared between the video transect survey and that of Fonseca and Bell (1998). After natural log + 1 or arcsine (for percentage of organic content) transformation, each attribute was regressed (Proc GLM [general linear model], SAS 1989) on REI by hydrodynamic regime and data type (grid-sampled, video transect) (Analysis IX, Table 3). These same ecological attributes were analyzed under principal components analysis (PCA) after transformation (ln[value + 1]; except for data presented as ratios; SAS 1989) to determine relationships among ecological attributes (also Analysis IX, Table 3).

Shoaling effects

Because only fetch is used in the computation of REI, we conducted a test to evaluate the relative importance of including shoaling effects on the REI-based predictive models. Shoals will act to attenuate wind-generated waves, meaning that even a site exposed to a long fetch might not result in high wave exposure if a shoal existed in close proximity to that site. One of the seven study areas was selected that featured abrupt REI gradients (Fig. 2a) and had extensive shoaling around a small isolated island (Dredge Island). Recent placement of dredge material on the island had changed its shoreline configuration as well as adding to the adjacent shoals, which had not been incorporated into the NOAA shoreline data layer used for the REI computation. Therefore, the Dredge Island was remapped in early May 1997 using a Trimble Pro-XL differential GPS. Thirty-six locations, variably spaced so as to capture visually obvious geometric variation in the island's outline (as viewed onsite) were located with ~1 m accuracy. This time, the outline of the island was defined to include subtidal shoals to a depth determined by the shallowest extent of the local seagrass bed (−0.22 m MSL). A new REI grid, which included the three video transects immediately adjacent to Dredge Island and which was situated largely in the lee of the strong northeast fetch, was computed based on the new, shoal-defined outline of Dredge Island. These new, shoal-based REI values were merged as before with the previously surveyed video transects (Fig. 2b). New regressions, PCA, and a logit function were computed for the data contained in only these three video transects next to the island (Analysis X, Table 3) and then compared to the original analyses (Analyses I–IV, Table

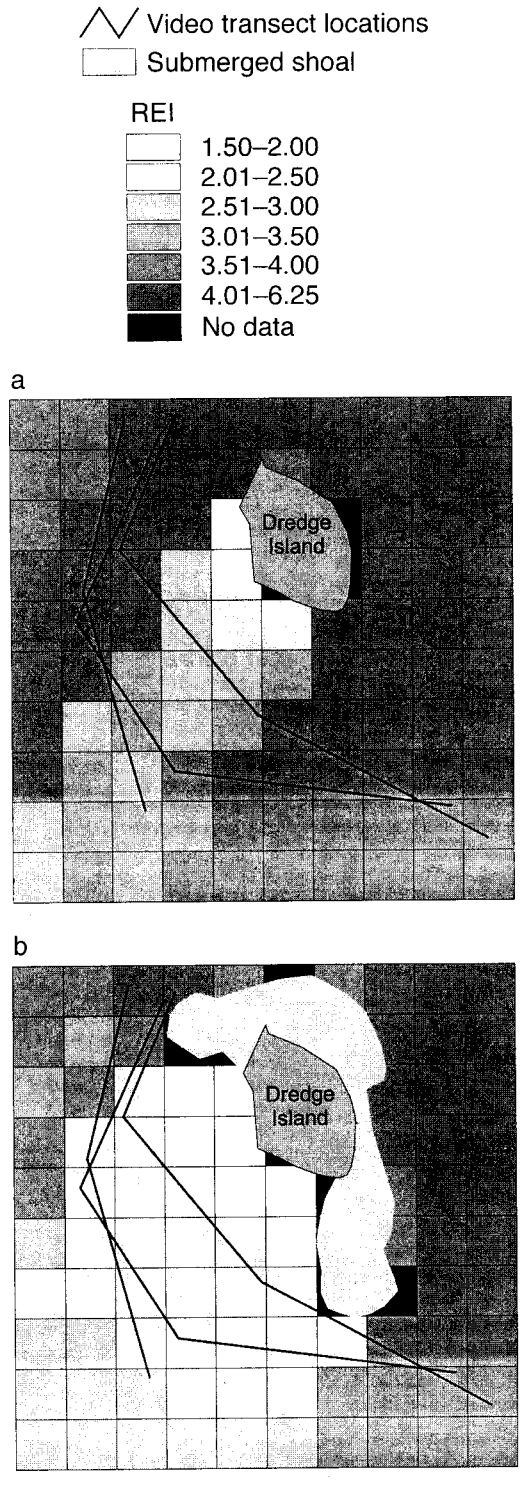

FIG. 2. (a) Dredge Island relative (wave) exposure index (REI) grid based on a shoreline shape derived from the emergent portion of the island. (b) New REI grid based on a May 1997 survey including subtidal shoals acting as shoreline for interpreting fetch distances. REI is expressed in thousands (i.e., $\times 10^{-3}$). Pixel sizes are 1 ha^2.

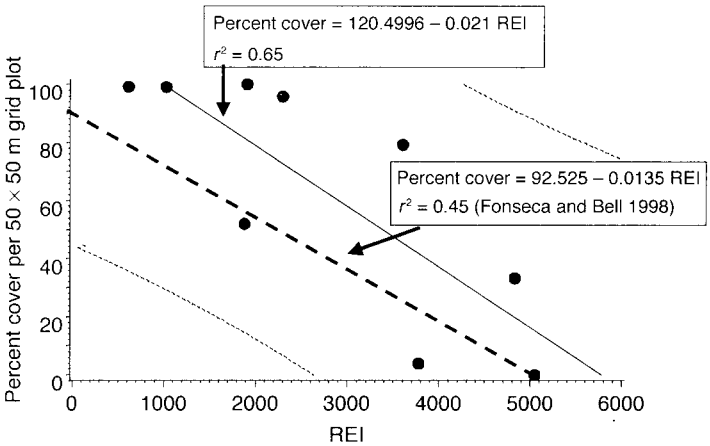

FIG. 3. Comparison of regressions of percent cover on relative (wave) exposure index (REI, computed in thousands) from Fonseca and Bell (1998) (dashed line) with spring 1995 surveys of nine representative sites (solid line and 95% confidence limits).

3). These two groups of analyses were then compared and qualitatively assessed for the potential importance of intervening shoals as an influence on REI modeling.

RESULTS

Coherence of the coverage–REI relationship over time

Percent cover of the 50 × 50 m grid sites resurveyed in May 1995 was regressed on REI for that sampling time. This regression produced a relationship similar to that found at the same sites in 1991–1992 by Fonseca and Bell (1998; Fig. 3), with cover decreasing with increasing REI. The most obvious trend was for slightly greater seagrass cover per unit REI in 1995 than in 1991–1992.

Predicting seagrass cover from video transect and grid data

Seagrass cover varied with water depth, but the distribution of sampling effort differed between the video transect and grid data. The grid-sampled (50 × 50 m grid) data, which was collected by walking the site, had sampling effort distributed across a greater range of depths, but concentrated at shallow areas (Fig. 4). Video transect data, which were collected using a boat and ranged far beyond the boundaries of the 50 × 50 m grids, tended to have greater sampling effort in deeper areas (Fig. 4). Seagrass cover was greatest between −0.75 and −1.0 m MSL as well as at 0 MSL (Fig. 5), possibly reflecting the relative depth preferences of the two seagrass species. It is likely that within this range,

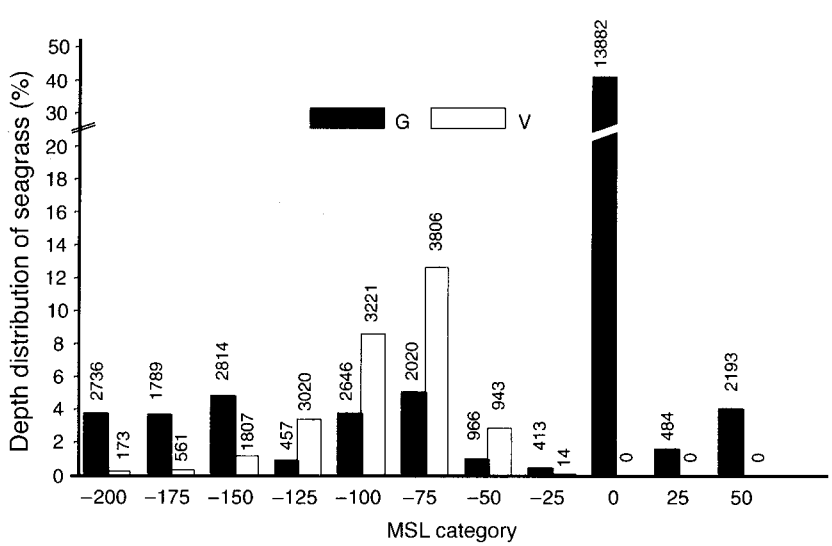

FIG. 4. Depth distribution of seagrass by mean sea level (MSL) water depth (in centimeters) for surveys conducted in 1991–1992 (50 × 50 m grid, G) vs. 1995 (video transect, V). Numbers above bars are the number of 1-m^2 observations in that category.

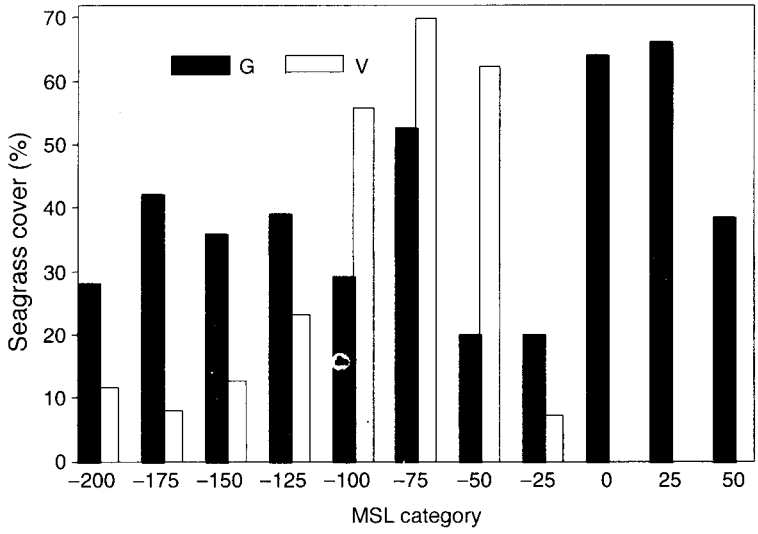

FIG. 5. Percent cover of seagrass by mean sea level (MSL) water depth (in centimeters) for surveys conducted in 1991–1992 (50 × 50 m grid, G) vs. 1995 (video transect, V).

the deeper areas would be dominated by a *Zostera–Halodule* mix while the shallower sites, particularly those near 0 MSL, would be dominated almost exclusively by *H. wrightii.* Video transects ranged also onto areas of higher REI than that of the grid-sampled sites (Fig. 6). As might be expected, low REI areas, characterized by more continuous, low relief beds (dominated by *H. wrightii*), appear to be easily identified by video transect methods, as evidenced by the very high r^2 value in Table 4. We posit that this relationship exists simply because a more continuous bed likely has a higher probability to be detected and recorded by a transect.

The effect of unequal sampling effort among depths and REI by each survey method was particularly apparent when comparing percent cover using the seven REI categories (Analysis VII, Table 3). Grid-sampled data displayed a significant ($P < 0.05$) negative correlation of percent cover with REI, whereas the comparatively small sample size in low REI sites using the video transect data apparently resulted in coverage being underestimated at REI $< 3 \times 10^6$ REI (Fig. 7a). When the relationship between percent cover and REI was examined for only high exposure sites ($>3 \times 10^6$ REI), the regression lines for the two data types were similar and exhibited a significant negative correlation of percent cover with REI (Fig. 7b).

Logistic multiple regression performed over time,

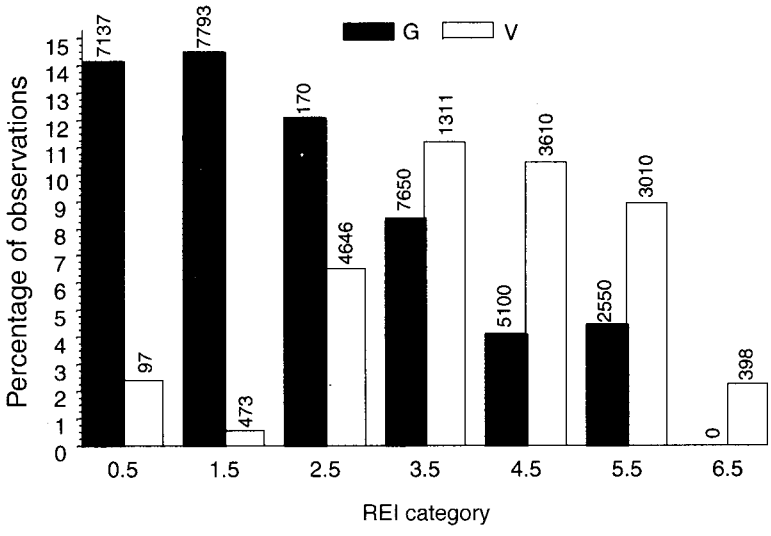

FIG. 6. Relative survey effort (percentage of 1-m^2 observations) by relative (wave) exposure index (REI) category for surveys conducted in 1991–1992 (50 × 50 m grid, G) vs. 1995 (video transect, V). Numbers above bars are total numbers of observations.

TABLE 4. Logistic multiple regression for the probability that seagrass cover exists in a given square meter of bottom.

Analysis and description	Regression equations $\hat{p}$(grass = yes) = $a + b + c + d$					
	a	b	Correlation bc	c	d	Somer's D
For REI $\leq 3 \times 10^6$						
II. Grid sampling	−1.18 (9)	1.21×10^{-7} (54)	0.14	12.25 (32)	4.29	0.529
IV. Video transect	2.34 (13)	3.38×10^{-6} (20)	−0.28	8.24 (53)	−14.59	0.800
VI. Both	−0.06 (43)	9.94×10^{-7} (10)	−0.60	2.59 (47)	−0.28	0.586
For REI $> 3 \times 10^6$						
II. Grid sampling	−0.45 (0.5)	-7.98×10^{-7} (26)	0.12	4.23 (4)	4.31	0.313
IV. Video transect	0.24 (34)	-1.34×10^{-7} (16)	−0.19	2.88 (54)	1.99	0.547
VI. Both	0.42 (22)	-4.87×10^{-7} (14)	−0.31	0.92 (8)	0.24	0.348
Complete data						
I. Grid-sampling	0.37 (7)	2.02×10^{-7} (25)	−0.25	3.22 (20)	−0.12	0.588 (0.279)
III. Video transect	2.7×10^{-5} (30)	-1.80×10^{-7} (16)	−0.09	3.14 (52)	0.15	0.598 (0.584)
V. Both	0.31 (10)	-3.42×10^{-7} (23)	−0.13	1.38 (12)	0.32	0.372 (0.360)
Case study, Dredge Island						
X. Emergent shoreline		-5.01×10^{-7} (26)		0.0424 (77)	7.0868	0.633
X. Shoreline plus submerged shoals		-8.35×10^{-7} (54)		0.0404 (73)	7.0066	0.718

Notes: In the regression equations, a = survey date, b = relative (wave) exposure index (REI), c = water depth relative to mean sea level (MSL), and d = intercept. Somer's D is the rank correlation index. In the columns for a, b, and c, values in parentheses are the percentages of Somer's D explained by each independent variable alone; in the Somer's D column, the numbers in parentheses resulted from a reanalysis of the data using only values where REI and MSL overlapped between the two sampling methods (grid-sampling and video transect).

REI, and MSL data (autocorrelation of REI and MSL; $r = -0.25$) revealed that for the complete data set (both energy regimes combined) prediction strength (Somer's D) of seagrass cover by both video transect and grid-sampled data was almost identical, suggesting that sampling disparities among shallow and deep areas and low and high REI areas for the two sampling methods had compensated for each other within the model. However, within both the high- and low-energy classifications, video transect-derived models had somewhat greater prediction strength than grid-sampled data (Table 4). For each survey method, model prediction strength was generally greatest in low-energy areas and less in high-energy areas, the latter being approximately equal to that of the complete data set (combined high- and low-energy areas). Overall, there was no obvious pattern as to whether REI or MSL (and survey date, the effect of which was blocked by forcing it into the model), accounted for most of the model variance. There was a tendency for REI to account for more model variance in grid-sampled sites than in video transect sites; the opposite was true for MSL that accounted for more model variance in video transect than grid-sampled sites. The combined data set of both video transect and grid data had the lowest D values, whether considered by or irrespective of energy regime (Table 4).

We reanalyzed the "complete data" for just those portions of the data where REI and MSL overlapped between the two sampling methods; D value dropped in all cases: from 0.588 to 0.279 (grid-sampled), from 0.598 to 0.584 (video transect), and from 0.372 to 0.360 (both). This indicated that the lack of overlap of the data sets was not adversely affecting prediction strength and that the grid-sampled prediction actually depended strongly upon data from the higher REI and deeper MSL sites that were surveyed. Variation accounted for by survey date may reflect the influence of the two dominant seagrass species (*Z. marina* and *H. wrightii*) having peak abundances at different times of the year. But when considered by energy regime, grid-sampled sites had a positive correlation of REI with MSL, while video transect sites had a negative correlation, as might be expected with the relative proportion of sampling effort for these variables between the two survey methods (see Figs. 4, 6 and 7a, b). When combined, video transect data dominated the sign of the correlation negative between REI and MSL.

For high energy areas (REI $> 3 \times 10^6$) the logistic-based assessment yielded similar trends as simple REI-based models (Fonseca and Bell 1998); seagrass coverage decreased with increasing REI (Table 4). This is consistent with the linear regressions of coverage on REI (Fig. 7b). Low-energy areas (REI $< 3 \times 10^6$) displayed the opposite effect, which again was consistent with Fig. 7a, in that coverage increased with REI, a response we attribute to the dominance of shallow water sites in that portion of the sampling effort. Similarly, MSL was positively correlated with coverage in all cases. To generalize, the combined effects of both water depth and REI on the probability of seagrass coverage are shown in Fig. 8, where the probability of cover declines both as a function of increased REI and increased water depth.

Scale dependence of seagrass cover

In general, a much larger spatial extent of scale dependence for seagrass coverage was detected using the video transect data than was evidenced using the grid-

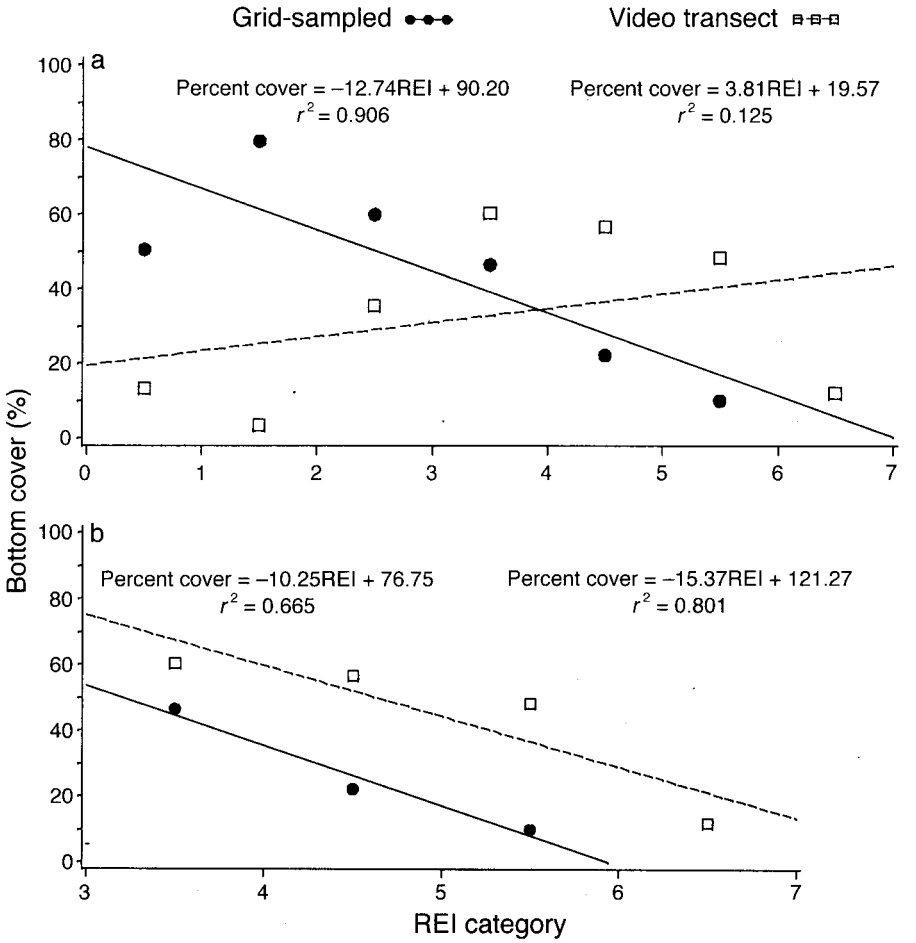

FIG. 7. (a) Percent bottom cover for surveys conducted at 1-m resolution in 1991–1992 (50 × 50 m grid-sampled) vs. 1995 (video transect). All relative wave exposure index (REI) categories are based on midpoints in increments of 1×10^6. (b) Percent bottom cover for surveys conducted at 1-m resolution in 1991–1992 (50 × 50 m grid-sampled) vs. 1995 (video transect). All REI categories are based on midpoints in increments of 1×10^6. The regression is for REI value categories $> 3 \times 10^6$.

sampled 50 × 50 m data alone. For three of the video transect data collections, variation in seagrass cover as a function of distance between samples never stabilized with spatial extent. Two sites (HIH1 and NRH1) exhibited semivariance stabilization (scale dependence) in the range of 300–450 m (Fig. 9a). Only two sites (BR2 and DAVIS) showed signs of reaching scale independence within the range of the original 50 × 50 m surveys (Fig. 9b; although DAVIS was a new site and had not been previously surveyed). DAVIS also had the shortest transect distances of any video transect sites, only 3–4 times that of the grid-sampled sites. One site (BR2) was previously found by Fonseca (1996*b*) to reach scale independence (using measures of topography, not cover) at the 18-m extent and approached scale independence at ~20 m using the coverage data (Fig. 9a). This demonstrates the well-known linkage of seagrass coverage with topography (sensu Fonseca et al. 1983). For the grid-sampled data, which was based on an assessment of 50 × 50 m areas, the spatial extent over which scale-dependent changes in seagrass cover occurred as computed by semivariogram analysis averaged 10.4 m (Fig. 9b, Analysis VIII).

Modeling ecological attributes across hydrodynamic gradients

Ecological attributes of the seagrass beds, obtained from the 1-m^2 quadrat samples from both grid data (50 × 50 m sites) and video transects were regressed on REI (Table 5). An already low prediction strength was lower still for three of four ecological attributes using data from within the quadrats located on video transects, as compared to those collected from the 50 × 50 m grids. There was no relationship found for aboveground biomass with REI using either grid sampling or video transects (Table 5). In most cases, however, the slopes of the regression lines among grid-sampled data and transects were similar although the data spread was large and prediction strength (r^2) was very low.

When correlations were significantly different from

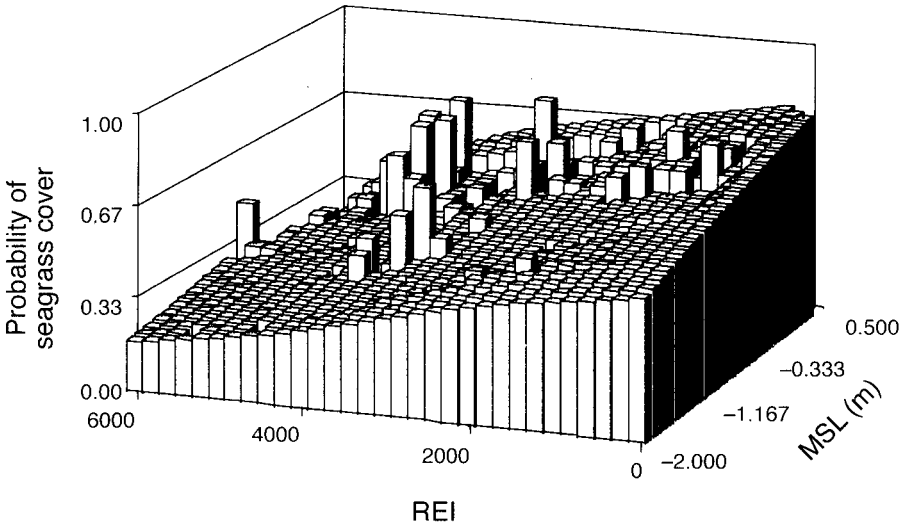

FIG. 8. Results of logistic multiple regression using combined video transect and grid-sampled data to predict the probability of seagrass cover (at 1-m resolution) from the relative (wave) exposure index (REI) and water depth (expressed in meters, relative to mean sea level, MSL).

zero, sediment organic matter (OM) from both grid-sampled and video transect sources was negatively correlated with REI, whereas shoot density and belowground biomass were positively correlated (Table 5). Grid-sampled data displayed the strongest (negative) correlation with REI, whereas only the video transect data for REI $> 3 \times 10^6$, which contained more high-exposure sites as compared to the grid-sampled sites, produced a significant but weak (negative) regression of sediment OM on REI. Similarly, prediction strength for belowground biomass was lower using video transect data as compared with grid-sampled data (Table 5). Video transect data displayed no correlation of REI with either shoot density or aboveground biomass.

Regressions were also computed for the four ecological attributes as a function of corrected water depth (MSL). Water depth accounted for little variation in most ecological attributes although in one instance it displayed a significant correlation with shoot density (shoot density $= -0.0297 \times$ MSL $+ 8.907$; $r^2 = 0.434$, $P < 0.05$). When the four ecological attributes were tested under one-way ANOVA for differences among high- and low-energy regimes (not shown), the only significant difference ($P < 0.05$) was found for shoot density, which was higher in the high- vs. the low-energy sites (not shown).

Using principal components analysis (PCA) of the four dependent variables obtained from quadrats taken along the video transects, three principal components had eigenvalues higher than one (Table 6; see also Table 3, Analysis IX), accounting for ~90% of the standardized variance. The first three principal components accounted for ~38, 27, and 25% of the standardized variance, respectively. Seagrass biomass (above- and belowground) loaded primarily on the first eigenvector, sediment OM loaded most heavily on the second eigenvector, and shoot density loaded best on the third (Table 6). Classification of sites as high (REI $> 3 \times 10^6$) and low (REI $< 3 \times 10^6$) energy regimes indicated no particular grouping by regime (Fig. 10), a departure from that reported by Fonseca and Bell (1998) for the 50 × 50 m grid-based data, where strong grouping into low- and high-REI regimes occurred.

Shoaling effects on prediction of seagrass cover and ecological attributes

The REI grid around Dredge Island was recomputed based on new ground-truthing of the shoal areas (Fig. 2b; see also Table 3, Analysis X). The original data from the three video transects adjacent to the island were merged with the new REI grid values. Classification of percent cover by REI exposure category was computed using both the original and new REI grid values, but just for these three transects. Using the original REI grid, the regression equation calculated for percent cover and REI was: % cover $= -7.573 \times$ REI (original) $+ 79.12$; $r^2 = 0.55$, and using the new REI grid, the equation was: % cover $= -11.921 \times$ REI (new) $+ 77.58$; $r^2 = 0.66$, a 0.11 increase in r^2 and a steeper regression slope. The regression of sediment OM on REI data obtained from the three video transects was not significant using the original REI grid but REI accounted for ~52% of OM variation using the new REI grid (not shown).

The logit function was also recomputed using both the old and new REI grids for these three video transects (Table 4). By accounting for shoal effects, Somer's D increased from 0.633 to 0.718 and REI could account for 28% more of the model variance; MSL consistently accounted for almost 75% of model var-

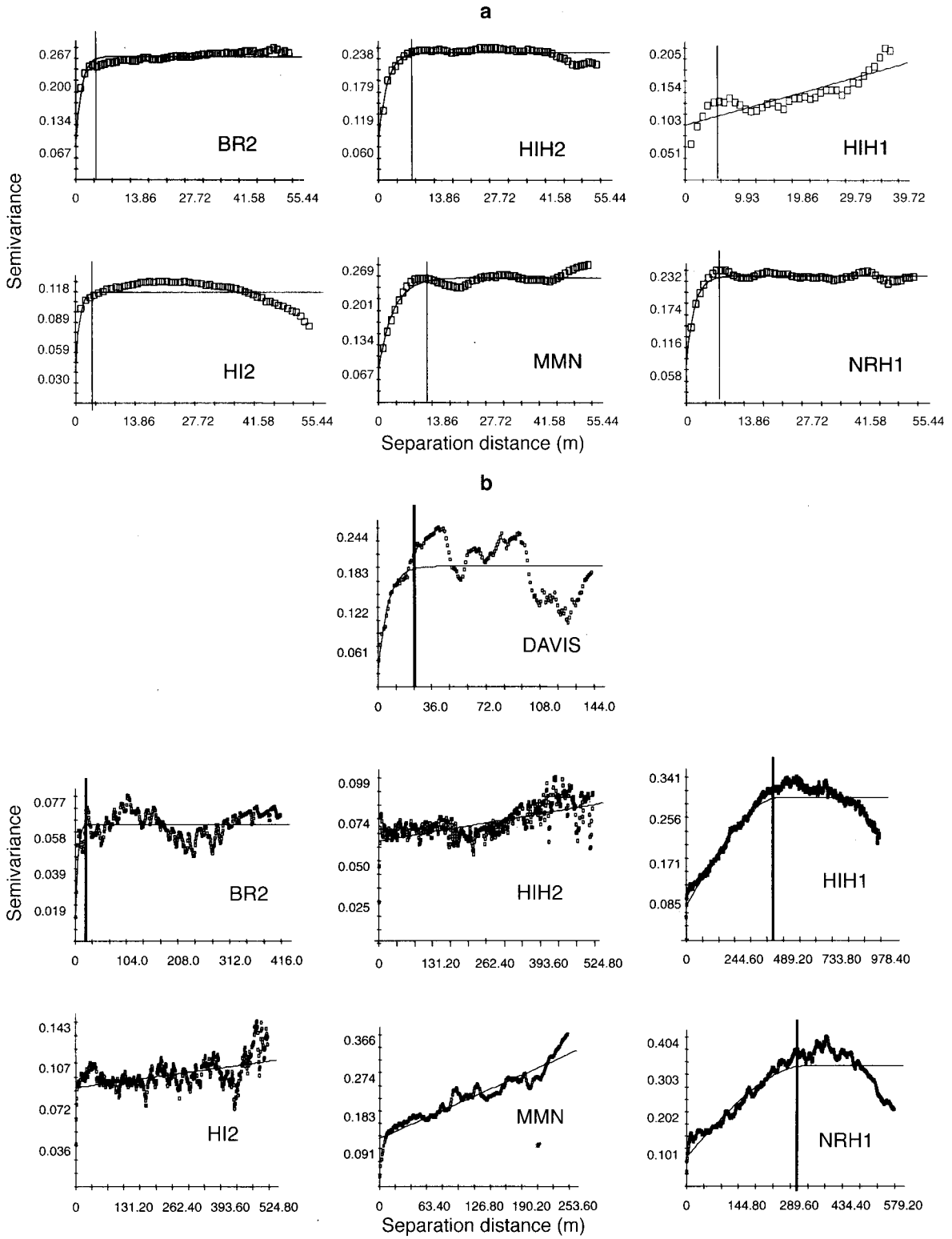

FIG. 9. (a) Best-fit semivariogram models of binomial seagrass coverage data, by site, computed using GS+ (1994) on 1-m resolution data, as a function of the total length of the video transect. (b) Best-fit semivariogram models of binomial seagrass coverage data, by site, computed using GS+ (1994) on 1-m resolution data, as a function of the total area of the 50 × 50 m grids that are common to both the video transect and grid surveys. The Davis site was not sampled in the 1991–1992 surveys. Horizontal axis (separation distance) is transect distance in meters. Vertical lines (where present) indicate approximate spatial distance where coverage semivariance stabilized. Note difference in the extent of the separation distances between (a) and (b).

TABLE 5. Comparison of regression statistics (f[relative wave exposure index, REI]) for the four variables common to quadrat-derived data from both the 50 × 50 m grid study and the present video transect-based study.

Variable (Y)	Project name	$Y = mX + b$	N	r^2
Percentage of organic matter	50 × 50 m grid	-4.19×10^{-7} REI + 2.738	68	0.37
	50 × 50 m grid, REI >3 × 10^6	-7.03×10^{-8} REI + 1.264	26	0.008 ns
	Video transect	-7.42×10^{-8} REI + 1.631	73	0.065 ns
	Video transect, REI >3 × 10^6	-5.14×10^{-7} REI + 3.781	34	0.34
Shoot density	50 × 50 m grid	2.39×10^{-4} REI + 1547.9	68	0.14
	50 × 50 m grid, REI >3 × 10^6	5.58×10^{-4} REI + 3.89	26	0.04
	Video transect	1.39×10^{-4} REI + 1026.9	73	0.04 ns
	Video transect, REI >3 × 10^6	2.47×10^{-4} REI + 2983.07	34	0.033 ns
Belowground biomass	50 × 50 m grid	4.50×10^{-5} REI + 100.53	68	0.23
	50 × 50 m grid, REI >3 × 10^6	5.89×10^{-5} REI + 33.78	26	0.056 ns
	Video transect	1.60×10^{-5} REI + 56.17	73	0.085
	Video transect, REI >3 × 10^6	2.07×10^{-7} REI + 3.685	34	0.024 ns
Aboveground biomass	50 × 50 m grid	-4.91×10^{-7} REI + 56.364		ns
	50 × 50 m grid, REI >3 × 10^6	-3.89×10^{-6} REI + 70.639		ns
	Video transect	2.91×10^{-8} REI + 22.233	73	0.028 ns
	Video transect, REI >3 × 10^6	1.41×10^{-8} REI + 45.12	34	0.001 ns

Notes: The abbreviation "ns" indicates a regression slope not significantly different ($P > 0.05$) from zero. N = sample size. These are results for Analysis IX, Table 3.

iance. When multivariate (PCA) analysis was recomputed for the old and new REI values, using these three transects, no changes in distribution of loading among principal components was found as compared with the previous analysis using all observations (not shown).

DISCUSSION

Predicting seagrass cover from video transect and grid data

Temporal coherence of the cover–REI relationship.—In order to proceed with the comparison of the video transect and the grid-sampled data sets, we had to deal with a 3-yr separation of the two surveys. We approached this problem by evaluating the seagrass cover–REI relationship to determine if it remained as described by Fonseca and Bell (1998). When the regression lines of percent cover on REI from the two studies were compared, the nature of the relationship was similar. What is noteworthy was that more seagrass was found per unit increase in REI in 1995 as opposed to the earlier surveys (Fig. 3). The coherence of the percent cover–REI relationship for the grid-sampled sites between 1991–1992 and 1995 suggest that this relationship has been maintained and that video transect surveys of the areas in 1995 should have encountered beds with as much or more cover as in existence in 1991–1992. Moreover, this similarity in the relationship between REI and seagrass coverage over time supports the notion that the relationships derived by Fonseca and Bell (1998) were not simply an artifact of a single sampling effort.

TABLE 6. Principal-components (PC) analysis of North Carolina seagrass habitat attributes based on video transect quadrat-derived samples.

Attribute	PC1	PC2	PC3
Sediment percentage of organic matter content	−0.160	*0.892*	0.240
Shoot density	0.167	−0.199	*0.963*
Aboveground biomass	*0.658*	0.389	−0.085
Belowground biomass	*0.717*	−0.112	−0.092

Notes: Values in italic type are eigenvectors with strong loading for individual attributes. Percentages of contributions of principal components were 38.6%, 26.8%, and 24.6%, and the cumulative percentages of variance accounted for by addition of the principal components were 38.6%, 65.4%, and 90.1% for PC1, PC2, and PC3, respectively.

Despite the differences in sampling strategies between the two survey types, the multivariate analysis (PCA) of the video transect data revealed some similarities to the findings of Fonseca and Bell (1998) that were derived from the discrete 50 × 50 m grid-sampled sites. As was seen by Fonseca and Bell (1998), biomass values here loaded separately from sediment organic content. However, shoot density loaded on yet another eigenvector whereas for Fonseca and Bell (1998) it loaded with biomass. This change in loading may be because in the grid-sampled sites, shoot density was significantly correlated with REI (Table 5) whereas it was not along video transects. This means that changes in shoot density would not necessarily follow that of an REI-correlated factor such as belowground biomass. We suspect that separation of these factors onto different eigenvalues may arise because samples taken along video transects were less apt to be spatially autocorrelated (see *Predicting seagrass bed attributes* and *Influence of scale dependence on predictions*).

Predicting seagrass bed attributes.—When comparisons between the video transect and grid-sampled sites were made, large-scale features of the landscape, such as patches several meters in width that were visually apparent in the 1995 aerial photography (see Plate 1), appeared to be best quantified by sampling over a large spatial extent (hundreds of meters or greater). Conversely, the ecological attributes of biomass, shoot density, and sediment composition, attributes of the seagrass beds that would not be readily detectable from

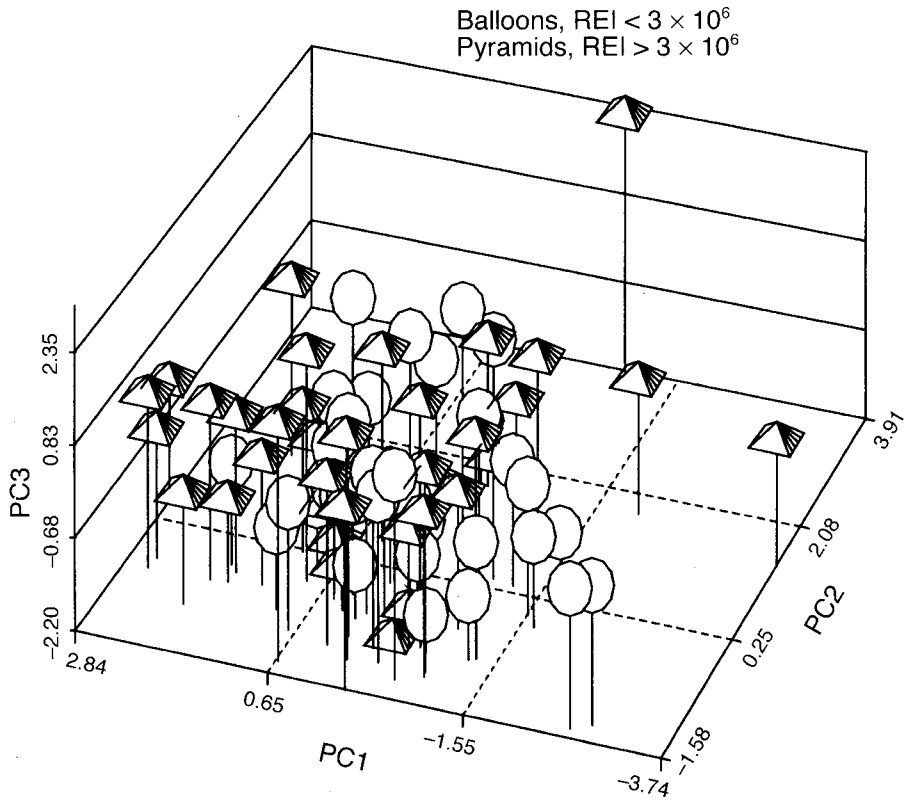

FIG. 10. Three-dimensional plot showing eigenvalues for the first three significant principal components (PC) computed for video transect (1995), quadrat-derived data on shoot density, above- and belowground biomass, and percentage of sediment organic content. Balloons represent sites with relative (wave) exposure index value categories $> 3 \times 10^6$ (based on midpoints in increments of 1×10^6).

aerial photography, were best characterized by sampling over a shorter spatial extent (1–50 m). Therefore, only seagrass cover showed the potential for being scaled to coarser levels of representation with statistical predictability. Specifically, when stratified by REI, data collected on seagrass coverage over a larger spatial extent at each site (i.e., video transect data) improved prediction strength over that collected from the 50 × 50 m grid-sampled sites (Table 4) by ~38%.

However, when combined across energy regimes, both data collection methods (video transect and grid sampling) were almost equal in their ability to predict seagrass cover, despite seagrass cover exhibiting a loss of scale dependence at ~300 m, nearly four times longer than the longest dimension in the grid-sampled sites (where scale dependence of coverage was lost at ~10 m). We posit that the limited spatial extent of coverage sampling at a grid-sampled site was compensated by having sampled many 50 × 50 m sites across the full local gradient of hydrodynamic settings as well as seagrass coverage (also see Fonseca and Bell 1998). Because the video transect data captured a larger range of scale-dependent variation in seagrass cover at each sampling site, a somewhat greater predictive strength should have been derived from these data, as was the case (Table 4). Conversely, data collected on seagrass ecological attributes were generally better predicted (albeit with very low r^2) by grid-sampled data. These grid-sampled data were collected with greater local replication (three samples per 50 × 50 m grid) and correlated with REI and water depth values derived over a smaller geographic extent than that of the video transect data. It may be that because the full extent of these grid-sampled sites was well within the range of spatial scale dependence detected using the video transect data, the attributes were spatially autocorrelated, contributing to a somewhat higher r^2. With video transects, the sampling locations of throwtraps were sometimes spaced hundreds of meters apart and, therefore, were less susceptible to spatial autocorrelation. Therefore, if seagrass coverage surveys are anticipated to occur over a range of REI and coverage levels, either grid-sampled or video transect surveys would be effective methodology, but only if care is taken to avoid biasing the sample collection towards certain water depths, particularly with grid-sampling (Table 4). However, over large areas, especially where patchy seagrass beds will be encountered, the video transect approach should yield better results.

Influence of scale dependence on predictions.—Es-

tablishing relationships among ecological variables using a cross-scale comparison of data (i.e., data collected at differing spatial extent) is frequently a problem in field studies (sensu Cao and Lam 1997). Here, when seagrass coverage taken from grid-sampled sites was averaged at the same scale as that of the associated REI computation (50 × 50 m), a strong correlation with REI was found. However, when computing a regression with coverage predicted at 1 m but REI computed >1 ha (Table 2), prediction strength was much less. Another example of cross-scale comparisons eroding predictive strength may be found when the Somer's *D* values for this study (which ranged from 0.313 to 0.80) were compared with the findings of Narumalani et al. (1997). Narumalani et al.'s data on a freshwater ecosystem all were collected at the same spatial resolution and had Somer's *D* values >0.90, whereas coverage and water depth data here were collected with much higher spatial resolution than was the computation for REI (one value for each 0.25-ha grid-sampled site and 1.0-ha resolution for transects). These data suggest that the prediction of seagrass coverage as a function of hydrodynamic setting can be improved not only by increasing the spatial extent of sampling at a fixed resolution (1 m) as was done with the video transects, but by ensuring that data for both dependent (e.g., percent cover) and independent (e.g., REI) variables are averaged over similar scales (spatial extent and resolution).

Influence of sampling protocol.—Distribution of effort between the two sampling techniques also contributed somewhat to prediction strength. Here, sampling efforts were obviously biased by collection protocols. All of the grid-sampled sites were surveyed by walking and systematically observing each 1 m^2 of the site for seagrass cover (Fonseca and Bell 1998). Sampling by walking probably biased site selection towards shallow sites easier to traverse on foot, and these sites happened to range to the low end of the REI. By contrast, the video transect data collection occurred in deeper areas where the boat could maneuver and were associated with the higher end of the REI. Consequently, when just the higher REI ranges were examined, the correlation between percent cover and REI category was improved for the video transect data (Fig. 8b). Interestingly, when these coverage data were reanalyzed under logistic regression using only portions of the data sets where REI and MSL values overlapped, the only substantive change in prediction strength was a severe erosion of prediction strength using grid-sampled data (Table 4). Limiting the analysis to overlapping data ranges eliminated the higher REI sites from consideration and revealed the importance of having representative sampling across REI (and by correlation, MSL) for these sampling sites.

The bias in sampling REI and water depths among the two data types also may have revealed the sensitivity of seagrass coverage to the interplay of wave effects and water depth. Because water depth determines the amount of wind wave energy that reaches the seafloor, shallower sites should experience greater and more frequent wave-induced water motion than deeper sites. Even though the grid-sampled sites tended to be located in more protected settings and had a generally lower REI, they were also shallower (than video transect data), and the logit function tended to reveal a greater effect of REI at these sites as compared with video transect sites. The generally higher REI (and deeper) video transect sites were influenced less by REI (Table 4). This sensitivity suggests that these models may be applicable in other geographic areas having similar ranges of REI and water depths, although this awaits confirmation.

Tests of these models in other locations should consider the potential embedded bias in the sampling by the two approaches. Predictions of cover for small, quiescent, shallow sites may be better based on the grid-sampled data, while deeper, more exposed sites spread over large areas were better described by the video transect-based model. As would be expected though, the greater the range of REI and MSL within the data set, the better the prediction, particularly when using the grid-sampled approach. Moreover, these models might also be better adapted elsewhere if local light attenuation coefficients were incorporated in place of depth data alone to predict accurately light availability to the plants. An estimation of light availability at the seafloor could be added by applying an attenuation coefficient to the depth data, allowing the light requirements of seagrass to enter the model.

Modeling ecological attributes across hydrodynamic gradients

Processes influencing predictive strength—matching scale with process.—Although there is strong correlative evidence that hydrodynamic setting, when examined at a coarse scale of resolution, influences a number of seagrass ecosystem functions (Taylor and Lewis 1970, Patriquin 1975, Orth 1977, Fonseca et al. 1983, Kirkman and Kuo 1990, Irlandi 1996, Fonseca and Bell 1998), our data collected for ecological attributes over a larger geographic extent (video transect sites) had an even lower predictive strength than those with already low r^2 values collected from smaller geographic extent (grid-sampled sites). Several ecological processes acting at scales closer to the 1-m scale may produce effects not detectable when sampling at coarser scales (i.e., this is the "Scale of Action"; Cao and Lam 1997). Grazing, sediment bioturbation, fishing gear impacts, local variations in sediment composition and chemistry, macroalgal or epiphyte biomass (influencing light availability), and perhaps most importantly, the recent history of extreme events (Gaines and Denny 1993, Fonseca et al. 2000*b*), may all act to disrupt the nexus of seagrass coverage, density, biomass, and sediment composition with wave exposure. All of

these factors are available to influence the seagrass beds near Beaufort. Conversely, correlations between seagrass cover and REI tended to improve as data were aggregated at spatial scales more like that at which wave effects (REI) were computed (1 ha; Fig. 8a, b), suggesting that indeed some factors influencing the seagrass bed attributes sampled at fine scales do not act, or at least are not detectable, at all scales and may be overridden by processes operating over coarser scales (Schoch and Dethier 1996). Likely candidates for the coarse scale factors in this study would be the wind field, represented as REI, and basin geomorphology, represented as water depth.

Another factor that may influence interpretation of these data is the known existence of a threshold in seagrass bed coverage, shape, and associated sediment composition that occurs near an REI of $\sim 3 \times 10^6$ for the seagrass beds near Beaufort (Fonseca and Bell 1998). Fonseca and Bell (1998) found that several ecological attributes displayed an abrupt transition near an REI of $\sim 3 \times 10^6$, including percent cover of seagrasses, seagrass bed perimeter-to-area ratio, and sediment organic content and percentage of silt–clay. Under this threshold model, because point samples of seagrass beds taken in association with video transects were mostly above the 3×10^6 REI threshold, only weak or nonexistent correlations with REI would be expected. The close agreement of the percent cover regressions between the two data types (Fig. 7b) when only the high REI data were regressed (contrast with Fig. 7a) further suggests that undersampling shallow, low REI sites in the video transect data poses significant problems with extrapolating those data across the REI threshold.

Shoaling effects on prediction of seagrass cover and ecological attributes

Local geomorphology emerged as being a critically important factor to incorporate into seagrass coverage modeling, likely irrespective of which sampling approach is employed. When submerged shoals were incorporated into a subset of the video transect data, better prediction was achieved for both the local depositional environment (increased prediction strength for sediment percentage of organic matter content) and the combined influence of REI and water depth on seagrass coverage probability. Therefore, it may be desirable to derive an REI computation that not only includes effective fetch, but also a weighting of the proximity of shallow water, especially if a critical shoal depth (where shoal effects become evident) could be determined. A model similar to that used in this study could be used to determine distance to these shoals and not just hard shorelines during GIS modeling. Adding these shoal data to improve prediction strength also points out the need for accurate bathymetric surveys. Unfortunately, bathymetric surveys may be quite out of date ($\sim$100 yr old for many areas near Beaufort) and are not often conducted over areas away from navigational channels where many seagrass beds occur, potentially diminishing their value in REI modeling.

Conclusions

The development of predictive vegetation modeling (sensu Franklin 1995) has only begun in seagrass ecosystems. However, we have shown that predicting the occurrence of seagrass cover based on physical setting is feasible. Such predictions of seagrass cover and associated landscape pattern are important for not only selecting potential restoration sites, but also for setting realistic management goals based upon unambiguous success criteria. For example, under a given REI and MSL, a site might be predicted to only achieve 50% cover, indicating that additional sites would be needed to generate a target level of restored seagrass acreage (Fonseca et al. 1998). Like landscape cover, predicting other restoration criteria, such as shoot density or biomass (Fonseca et al. 2000*a*), is critical for determining the recovery trajectory and computing lost interim resource services and civil penalties for damages to seagrasses.

The influence of sampling scale and survey method on the prediction of coverage and ecological attributes of seagrass beds dictates that resource managers and other environmental scientists need to choose sampling designs carefully in the Beaufort area and perhaps other like habitats. These data suggest that the prediction of seagrass coverage as a function of hydrodynamic setting can be improved not only by increasing the spatial extent of sampling at a fixed resolution (1 m), as done with the video transects, but by ensuring that data for both dependent (e.g., percent cover) and independent (e.g., REI) variables are averaged over similar scales (spatial extent and resolution). Moreover, low REI areas, characterized by more continuous, low-relief beds, appear to be easily identified by video transect methods. Similar conclusions were reached by Narumalani et al. (1997) in a study of submersed vegetation in a freshwater setting.

In this study, the small lack of overlap of REI and MSL between the two sampling approaches did not diminish predictive ability, although sampling across a broad range of REI and MSL values is obviously required to improve predictive modeling efforts. Large-scale features of the landscape such as patches several meters in width appeared to be best quantified by sampling over a large spatial extent (hundreds of meters or greater). However, unless one can somehow be certain that the full local range of seagrass bed cover is captured in the smaller scale sampling, contiguous sampling over a broad spatial extent (hundreds of meters) is the more appropriate strategy for detecting patterns of seagrass bed cover. Conversely, ecological attributes of the seagrass bed (biomass, shoot density, and sediment composition), features that are not readily detectable from aerial photography, were best character-

ized by sampling over a shorter spatial extent (1–50 m). Very localized conditions may have influenced patterns of seagrass community attributes, indicating that traditional sampling of ecological attributes at the 1-m scale is justified for organismal level studies of seagrass beds and perhaps their resident fauna as it may best approximate the "scale of action" for these attributes (sensu Cao and Lam 1997). Sampling over a broad spatial extent may then be the most parsimonious means of detecting changes in seagrass cover arising from anthropogenic disturbances, such as channel deepening or shoreline hardening, that may have in turn changed a site's exposure to waves and water depth (and light). Moreover, generalizing information about seagrass bed ecological attributes obtained from high-resolution samples (fine scale) taken over a broad spatial extent (coarse or landscape scale), as may occur with resource surveys and impact assessments, has the potential to be highly misleading, especially in patchy environments (sensu Schoch and Dethier 1996). When comparisons between the video transect and grid-sampled sites were made, only seagrass cover showed the potential for being scaled to coarser levels of representation with statistical predictability.

Finally, by linking this modeling to temporal dynamics of seagrass beds (Fonseca et al. 2000*b*), we anticipate that researchers will be able to both forecast and hindcast the consequences of extreme storm events on changes in seagrass cover and associated ecological attributes. Predictive capabilities of this kind will allow resource managers the ability to separate the influence of aperiodic extreme events on seagrass bed distribution and function from that of anthropogenic events.

Acknowledgments

We would like to thank Maurice Crawford, Monica Daniels, and Ed Townsend for their unflagging assistance in the field. David Colby provided crucial guidance on statistical analyses. Lisa Wood provided 1995 aerial photography. Valuable critical reviews were provided by Maurice Crawford, Carla D'Antonio, Randy Ferguson, Jud Kenworthy, M. A. R. Koehl, Pamela Matson, Gordon Thayer, and Wayne Sousa. Two anonymous reviewers and the endurance of the editor, P. Dayton, saved the manuscript. This work was funded by the NOAA Coastal Ocean Program, grant EHP-23 to the senior author, and the NOAA Beaufort Laboratory. This work was submitted in partial fulfillment of the Ph.D. requirements for the senior author in the Department of Integrative Biology, University of California, Berkeley, CA.

Literature Cited

August, P., J. Michaud, C. Labash, and C. Smith. 1994. GPS for environmental applications: accuracy and precision of locational data. Photogrammetric Engineering and Remote Sensing **60**:41–45.

Bell, S. S., M. S. Fonseca, and L. B. Motten. 1997. Linking restoration and landscape ecology. Restoration Ecology **5**: 318–322.

Bell, S. S., and M. O. Hall. 1997. Drift macroalgal abundance in seagrass beds: investigating large-scale associations with physical and biotic attributes. Marine Ecology Progress Series **147**:277–283.

Bell, S. S., M. O. Hall, and M. S. Fonseca. 1994. Evaluation of faunal and floral attributes of seagrass beds in high and low energy regimes: a geographic comparison. Pages 267–272 *in* K. R. Dyer and C. F. D'Elia, editors. Changes in fluxes in estuaries: implications from science to management. Olsen and Olsen, Fredensborg, Denmark.

Cambridge, M. L., A. W. Chiffings, C. Brittan, L. Moore, and A. J. McComb. 1986. The loss of seagrass in Cockburn Sound, Western Australia. Aquatic Botany **24**:269–285.

Cao, C., and N. S. Lam. 1997. Understanding the scale and resolution effects in remote sensing and GIS. Pages 57–72 *in* D. A. Quattrochi and M. F. Goodchild, editors. Scale in remote sensing and GIS. Lewis, New York, New York, USA.

Dobson, J. E., E. A. Bright, R. L. Ferguson, D. W. Field, L. L. Wood, K. D. Haddad, H. Iredate, J. R. Jensen, V. V. Klemas, R. J. Orth, and J. P. Thomas. 1995. NOAA coastal change analysis program (C-CAP) for regional implementation. NOAA Technical Report **NMFS 123**.

Ferguson, R. L., and K. Korfmacher. 1997. Remote sensing and GIS analysis of seagrass meadows in North Carolina, USA. Aquatic Botany **58**:241–258.

Ferguson, R. L., L. L. Wood, and B. T. Pawlak. 1991. SAV habitat in 1985 and 1988: Cape Lookout to Drum Inlet, North Carolina. Coastal Ocean Program chart. NOAA, Silver Springs, Maryland, USA.

Fonseca, M. S. 1996*a*. The role of seagrasses in nearshore sedimentary processes: a review. Pages 261–286 *in* C. Roman and K. Nordstrom, editors. Estuarine shores: hydrological, geomorphological and ecological interactions. Wiley, New York, New York, USA.

Fonseca, M. S. 1996*b*. Scale dependence in the study of seagrass systems. Pages 95–104 *in* J. Kuo, R. C. Phillips, D. I. Walker, and H. Kirkman, editors. Seagrass biology: proceedings of an international workshop, January 25–29, Rottnest Island, W. Australia, Australia. Faculty of Sciences, University of Western Australia, Crawley, Western Australia, Australia.

Fonseca, M. S., and S. S. Bell. 1998. The influence of physical setting on seagrass landscapes near Beaufort, North Carolina, USA. Marine Ecology Progress Series **171**:109–121.

Fonseca, M. S., B. E. Julius, and W. J. Kenworthy. 2000*a*. Integrating biology and economics in seagrass restoration: how much is enough and why? Ecological Engineering **15**: 227–237.

Fonseca, M. S., W. J. Kenworthy, and F. X. Courtney. 1996. Development of planted seagrass beds in Tampa Bay, Florida, USA: I. Plant components. Marine Ecology Progress Series **132**:127–139.

Fonseca, M. S., W. J. Kenworthy, and G. W. Thayer. 1998. Guidelines for the conservation and restoration of seagrasses in the United States and adjacent waters. NOAA Coastal Ocean Program, Decision Analysis Series number **12**.

Fonseca, M. S., W. J. Kenworthy, and P. E. Whitfield. 2000*b*. Temporal dynamics of seagrass landscapes: a preliminary comparison of chronic and extreme disturbance events. Pages 373–376 *in* G. Pergent, C. Pergent-Martini, M. C. Buia, and M. C. Gambi, editors. Proceedings of the Fourth International Seagrass Biology Workshop, September 25–October 2, 2000, Corsica, France. Biologia Marina Mediterranea, Istituto di Zoologia, Genova, Italy.

Fonseca, M. S., J. C. Zieman, G. W. Thayer, and J. S. Fisher. 1983. The role of current velocity in structuring seagrass meadows. Estuarine Coastal and Shelf Science **17**:367–380.

Franklin, J. 1995. Predictive vegetation mapping: geographic modelling of biospatial patterns in relation to environmental gradients. Progress in Physical Geography **19**:474–499.

Gaines, S. D., and M. W. Denny. 1993. The largest, smallest,

highest, lowest, longest, and shortest: extremes in ecology. Ecology **74**:1677–1692.

Ginsberg, R. N., and H. A. Lowenstam. 1958. The influence of marine bottom communities on the deposition environment of sediments. Journal of Geology **66**:310–318.

GS+. 1994. Geostatisics for the environmental sciences. Gamma Design Software, Plainwell, Michigan, USA.

Hine, A. C., M. W. Evans, R. A. Davis, and D. F. Belknap. 1987. Depositional response to seagrass mortality along a low-energy, barrier-island coast: west–central Florida. Journal of Sedimentary Petrology **57**:431–439.

Irlandi, E. A. 1996. The effects of seagrass patch size and energy regime on growth of a suspension-feeding bivalve. Journal of Marine Research **54**:161–185.

Irlandi, E. A., W. G. Ambrose, and B. A. Orlando. 1995. Landscape ecology and the marine environment: how spatial configuration of seagrass habitat influences growth and survival of the bay scallop. Oikos **72**:307–313.

Keddy, P. A. 1982. Quantifying within-lake gradients of wave energy: interrelationships of wave energy, substrate particle size and shoreline plants in Axe Lake, Ontario. Aquatic Botany **14**:41–58.

Kenworthy, W. J., J. C. Zieman, and G. W. Thayer. 1982. Evidence for the influence of seagrass on the benthic nitrogen cycle in a coastal plain estuary near Beaufort, North Carolina (USA). Oecologia **54**:152–158.

Kirkman, H., and J. Kuo. 1990. Pattern and process in southern Western Australian seagrasses. Aquatic Botany **37**:367–382.

Marba, N., and C. M. Duarte. 1995. Coupling of seagrass (*Cymodocea nodosa*) patch dynamics to subaqueous dune migration. Journal of Ecology **83**:381–389.

Murphey, P. E., and M. S. Fonseca. 1995. Role of high and low energy seagrass beds as nursery areas for *Penaeus duorarum* in North Carolina. Marine Ecology Progress Series **121**:91–98.

Narumalani, S., J. R. Jensen, J. D. Althausen, J. D. Burkhalter, and S. Mackey. 1997. Aquatic macrophyte modeling using GIS and logistic multiple regression. Photogrammetric Engineering and Remote Sensing **63**:41–49.

Orth, R. J. 1977. The importance of sediment stability in seagrass communities. Pages 281–300 *in* B. C. Coull, editor. Ecology of marine benthos. University of South Carolina Press, Columbia, South Carolina, USA.

Patriquin, D. G. 1975. "Migration" of blowouts in seagrass beds at Barbados and Carriacou, West Indies and its ecological and geological applications. Aquatic Botany **1**:163–189.

Quammen, M. L., and C. P. Onuf. 1993. Laguna Madre: seagrass changes continue decades after salinity reduction. Estuaries **16**:302–310.

Rastetter, E. B., A. W. King, B. J. Cosby, G. M. Hornberger, R. V. O'Neill, and J. E. Hobbie. 1992. Aggregating fine-scale ecological knowledge to model coarser-scale attributes of ecosystems. Ecological Applications **2**:55–70.

Robbins, B. D., and S. S. Bell. 1994. Seagrass landscapes: a terrestrial approach to the marine subtidal environment. Trends in Ecology and Evolution **9**:301–304.

Robbins, B. D., and S. S. Bell. 2000. Dynamics of a subtidal seagrass landscape: seasonal and annual change in relation to water depth. Ecology **81**:1193–1205.

Robblee, M. B., T. R. Barber, P. R. Carlson, M. J. Durako, J. W. Fourqurean, L. K. Muehlstein, D. Porter, L. A. Yarbro, R. T. Zieman, and J. Z. Zieman. 1991. Mass mortality of the tropical seagrass *Thalassia testudinum* in Florida Bay (USA). Marine Ecology Progress Series **71**:297–299.

SAS. 1989. SAS/STAT users guide, version 6, Fourth edition, Volume 2. SAS Institute, Cary, North Carolina, USA.

SAS. 1995. Logistic regression using the SAS system. Users guide, version 6, First edition. SAS Institute, Cary, North Carolina, USA.

Schoch, G. C., and M. N. Dethier. 1996. Scaling up: the statistical linkage between organismal abundance and geomorphology on rocky intertidal shorelines. Journal of Experimental Marine Biology and Ecology **201**:37–72.

Shore Protection Manual. 1977. US Army Coastal Engineering Research Center, Ft. Belvoir, Virginia, USA.

Taylor, J. D., and M. S. Lewis. 1970. The flora, fauna and sediments of the marine grass beds of Mahe, Seychelles. Journal of Natural History **4**:199–220.

Townsend, E. C., and M. S. Fonseca. 1998. Bioturbation as a potential mechanism influencing spatial heterogeneity of North Carolina seagrass beds. Marine Ecology Progress Series **169**:123–132.

Turner, S. J., J. E. Hewitt, M. R. Wilkinson, D. J. Morrisey, S. F. Thrush, V. J. Cummings, and G. Funnell. 1999. Seagrass patches and landscapes: the influence of wind–wave dynamics and hierarchical arrangements on spatial structure of macrofaunal seagrass communities. Estuaries **22**: 1016–1032.

Valentine, J. F., K. L. Heck, P. Harper, and M. Beck. 1994. Effects of bioturbation in controlling turtlegrass (*Thalassia testudinum* Banks ex Konig) abundance: evidence from field enclosures and observations in the Northern Gulf of Mexico. Journal of Experimental Marine Biology and Ecology **178**:181–192.

Zieman, J. C. 1972. Origin of circular beds of Thalassia (Spermatophyta: Hydorcharitacea) in south Biscayne Bay, Florida, and their relationship to mangrove hammocks. Bulletin of Marine Science **22**:559–574.